JOURNAL OF MATERIALS SCIENCE 37 (2002) 1611 – 1620

Phase relations in the system Cu-La-O and thermodynamic properties of $CuLaO_2$ and $CuLa_2O_4$

K. T. JACOB*, K. P. JAYADEVAN
Materials Research Centre and Department of Metallurgy,
Indian Institute of Science, Bangalore 560 012, India
E-mail: katob@metalrg.iisc.ernet.in

Phase relations in the system Cu-La-O at 1200 K have been determined by equilibrating samples of different average composition at 1200 K, and phase analysis of quenched samples using optical microscopy, XRD, SEM and EDX. The equilibration experiments were conducted in evacuated ampoules, and under flowing inert gas and pure oxygen. There is only one stable binary oxide La_2O_3 along the binary La-O, and two oxides Cu_2O and CuO along the binary Cu-O. The Cu-La alloys were found to be in equilibrium with La_2O_3. Two ternary oxides $CuLaO_2$ and $CuLa_2O_{4+\delta}$ were found to be stable. The value of δ varies from close to zero at the dissociation partial pressure of oxygen to 0.12 at 0.1 MPa. The ternary oxide $CuLaO_2$, with copper in monovalent state, coexisted with Cu, Cu_2O, La_2O_3, and/or $CuLa_2O_{4+\delta}$ in different phase fields. The compound $CuLa_2O_{4+\delta}$, with copper in divalent state, equilibrated with Cu_2O, CuO, $CuLaO_2$, La_2O_3, and/or O_2 gas under different conditions at 1200 K. Thermodynamic properties of the ternary oxides were determined using three solid-state cells based on yttria-stabilized zirconia as the electrolyte in the temperature range from 875 K to 1250 K. The cells essentially measure the oxygen chemical potential in the three-phase fields, $Cu + La_2O_3 + CuLaO_2$, $Cu_2O + CuLaO_2 + CuLa_2O_4$ and $La_2O_3 + CuLaO_2 + CuLa_2O_4$. Although measurements on two cells were sufficient for deriving thermodynamic properties of the two ternary oxides, the third cell was used for independent verification of the derived data. The Gibbs energy of formation of the ternary oxides from their component binary oxides can be represented as a function of temperature by the equations:

$$1/2\,Cu_2O + 1/2\,La_2O_3(\text{A rare-earth}) \rightarrow CuLaO_2$$

$$\Delta_{f,ox}G^\circ/\text{J mol}^{-1} = -4335 + 1.32\,T/\text{K}\ (\pm 45)$$

$$CuO + La_2O_3(\text{A rare-earth}) \rightarrow CuLa_2O_4$$

$$\Delta_{f,ox}G^\circ/\text{J mol}^{-1} = -19600 - 4.01\,T/\text{K}\ (\pm 240)$$

1. Introduction

Potential application of pure and doped lanthanide cuprates as electrodes, catalysts and superconductors provides the motivation for the study of their stability domains in the temperature-composition-oxygen potential space. The ternaries Cu-*Ln*-O form one of the bounding surfaces of the quaternary systems *Ln*-Ba-Cu-O, which contain high-T_c superconducting oxides. Phase relations and accurate thermodynamic data on bounding ternary systems are fundamental inputs for the calculation of the properties of complex higher order systems. As a part of systematic investigations into the bounding ternaries of the multinary systems containing superconducting oxides, isothermal phase relations in the ternary Cu-La-O have been elucidated, and accurate thermodynamic data on two ternary oxides $CuLa_2O_4$ and $CuLaO_2$ were determined using the solid-state electrochemical technique.

The stoichiometric compound $CuLa_2O_4$ has a tetragonal 14/*mmm* unit cell (K_2NiF_4-type) at temperatures

---

*Author to whom all correspondence should be addressed.

above 530 K with the *c*-axis perpendicular to the CuO_2 planes. At low temperature the structure is orthorhombic, described by the *Bmab* space group, resulting from the ordered tilting of the CuO_6 octahedra present in the structure around the tetragonal (1,1,0) axis [1]. There is some controversy regarding the nature of oxygen nonstoichiometry in $CuLa_2O_4$. Opila and Tuller [2] reported decreasing oxygen deficiency with increasing oxygen partial pressure ($\delta \propto P_{O_2}^{-1/6}$) in $CuLa_2O_{4-\delta}$ based on TGA measurements for $1323 > (T/\mathrm{K}) > 1073$ and $1 > (P_{O_2}/\mathrm{P^o}) > 10^{-4}$; throughout this article $\mathrm{P^o}$ is the standard pressure (0.1013 MPa). However, other TGA and electrical conductivity measurements as a function of oxygen partial pressure, notably by Nishiyama and coworkers [3, 4], indicate that the dominant defects in $CuLa_2O_4$ are oxygen interstitials and electron holes. Consequently, the chemical formula should be expressed as $CuLa_2O_{4+\delta}$. To resolve this dispute, the oxygen content of $CuLa_2O_4$ was measured as a function of oxygen partial pressure in this study at 1200 K.

More direct evidence for interstitials come from neutron diffraction studies. With the incorporation of excess oxygen in the 1/4, 1/4, 1/4 interstitial sites [5], ordered tilts are retained in $CuLa_2O_{4+\delta}$ at low temperature for $\delta < 0.06$. At higher values of δ, tilts are disordered; the structure remains orthorhombic with space group *Fmmm*. Electrostatic repulsion between oxygen ions or the number of available sites limits the density within an interstitial layer. Spacing between interstitial layers is governed by long-range strain energies. Wells *et al.* [6, 7] have suggested a sinusoidal modulation of the intercalated oxygen. Because the oxygen ions in $CuLa_2O_{4+\delta}$ remain mobile down to ~200 K, the phase diagram for $CuLa_2O_{4+\delta}$ can exhibit miscibility gaps. The phase separation into insulating oxygen-poor ($\delta = 0.01$) and semiconducting oxygen-rich ($\delta = 0.055$) phases has been reported below 290 K [8, 9].

The interstitial site for oxygen is between pairs of layers containing La and apical O atoms, directly above the in-plane oxygen as shown in Fig. 1. The oxygen ion in this site repels nearest neighbor apical oxygen ions and attracts La ions. A local tilt-flip of CuO_6 octahedron either below or above the excess oxygen ion creates a large interstitial position and maximizes the average distance between the extra oxygen ion and surrounding oxygen ions. Within a layer, the flipped tilt pattern propagates because of the shared corner oxygens. In turn, this creates an entire array of favorable interstitial sites in the same plane as the original interstitial oxygen.

Tretyakov *et al.* [10] have attempted to measure the Gibbs energy of formation of $CuLa_2O_4$ using a cell based on an oxide solid electrolyte. They were apparently unaware of the existence of $CuLaO_2$, and employed a non-equilibrium mixture of $Cu_2O + La_2O_3 + CuLa_2O_4$ at their measuring electrode. Chandrasekharaiah *et al.* [11] and Petrov *et al.* [12] have reported measurements on the Gibbs energies of formation of $CuLaO_2$ and $CuLa_2O_4$ and using similar electrochemical cells. Bularzik *et al.* [13] obtained a value of -19.30 (± 4.7) kJ $\mathrm{mol^{-1}}$ for the enthalpy of formation of La_2CuO_4 from binary oxides at 973 K using high-temperature solution calorimetry with molten $Pb_2B_2O_5$ as the solvent. The heat capacity of single-crystal and polycrystalline La_2CuO_4 has been measured by Sun *et al.* [14] from 110 K to 600 K using a differential scanning calorimeter (DSC). A cusp-shaped anomaly was observed in heat capacity at 523 K for a single crystal La_2CuO_4. This anomaly was somewhat smeared out in polycrystalline La_2CuO_4.

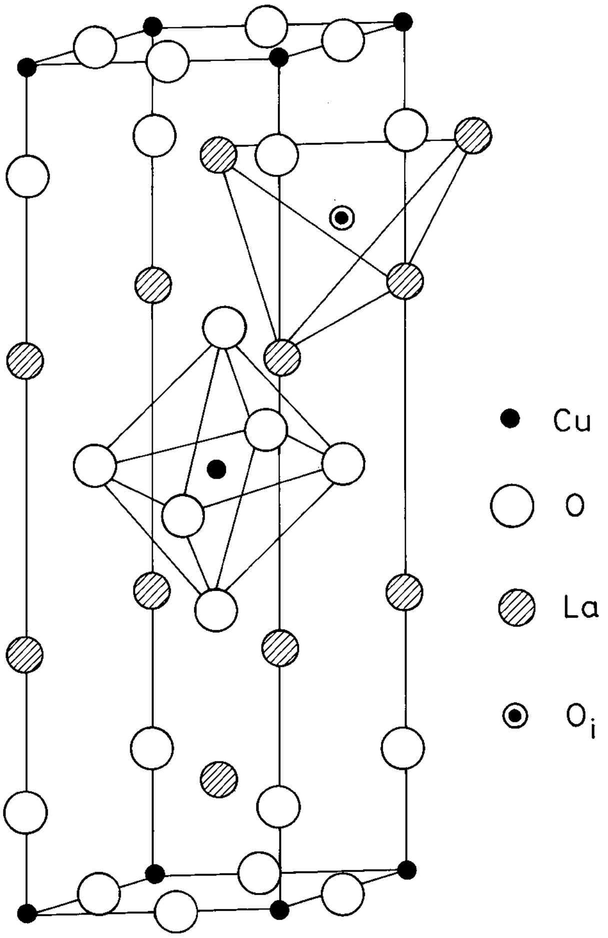

Figure 1 Tetragonal structure of $CuLa_2O_{4+\delta}$ with interstitial oxygen at 1/4, 1/4, 1/4 position.

Additional ternary oxides, $Cu_2La_2O_5$ and $Cu_7La_8O_{19}$, have been synthesized from CuO and La_2O_3 independently by Cava *et al.* [15] and Norrestam *et al.* [16] in the temperature range from 1260 to 1375 K in air or oxygen. Successful synthesis of these phases required rapid heating into the temperature stability region to prevent the formation of La_2CuO_4. It is claimed [15, 16] that the two compounds belong to the series $Cu_{4+n}La_{2+2n}O_{7+4n}$, with $n = 2$ and 3, respectively, where n is the number of edge-sharing CuO_6 octahedra between La_2CuO_4 slabs. Thermodynamic stability of these phases is an issue that needs to be addressed.

All previous electrochemical measurements were conducted using the conventional two-electrode cell design with air as the reference electrode. When there is a large difference in the chemical potential of oxygen between the reference and working electrodes, there is always a small electrochemical flux of oxygen through the solid electrolyte, from the electrode with higher oxygen potential to the electrode with lower oxygen potential. The trace hole conduction, and the consequent coupled migration of oxygen ions and electronic defects in the oxygen potential gradient, causes the flux [17, 18]. The oxygen flux can polarize multiphase solid electrodes and cause errors in the measured thermodynamic data. Introduction of a buffer electrode between the reference and measuring electrodes to absorb the flux has been recently shown to minimize polarization and generate high quality data [19–21]. In this study oxygen chemical potentials corresponding to two three-phase mixtures were measured using an advanced cell design incorporating a buffer electrode, with pure oxygen gas at a pressure of 0.1 MPa as the reference electrode.

2. Experimental procedure

2.1. Materials

The ternary oxides $CuLa_2O_4$ and $CuLaO_2$ were prepared from component binary oxides CuO, Cu_2O and La_2O_3, each of purity greater than 99.9%. The oxides were dried at 1100 K under a stream of pre-purified argon gas for ~40 ks. La_2O_3 used in this study had the hexagonal structure ($P6_3/mmc$) with lattice parameter $a = 0.3937$ and $c = 0.6130$ nm. For the synthesis of $CuLa_2O_{4+\delta}$, equimolar amounts of CuO and La_2O_3 were mixed, pelletized and heated at 1275 K in flowing dry oxygen for ~300 ks with three intermediate grindings. The compound was black in color and had the T-type (K_2NiF_4-type) structure. Copper has octahedral coordination and lanthanum is 9-coordinated in $CuLa_2O_{4+\delta}$. The ternary oxide $CuLaO_2$ was synthesized by heating pellets containing well-mixed stoichiometric amounts of Cu_2O and La_2O_3 in a zirconia crucible at 1273 K for a total period of 180 ks with two intermediate grindings. The zirconia crucible was sealed in an evacuated quartz ampoule to prevent oxidation of Cu_2O. Some copper wool was placed in the ampoule out of contact with the oxide pellet to absorb residual oxygen and prevent the oxidation of Cu_2O. After heat-treatment, the ampoule and pellet were quenched in liquid nitrogen or chilled mercury. Characterization using XRD showed the formation of single-phase compounds $CuLa_2O_{4+\delta}$ and $CuLaO_2$. The lattice parameters characterizing the orthorhombic unit cell of oxygen-rich $CuLa_2O_{4+\delta}$ ($\delta = 0.12$) were $a = 0.5341$, $b = 0.5405$ and $c = 1.3218$ nm. The unit cell parameters of rhombohedral ($R\bar{3}m$, $Z = 3$) $CuLaO_2$ were $a = 0.3831$ and $c = 1.7099$ nm in the hexagonal setting.

Ultra-high purity argon gas used to provide an inert atmosphere was first dried by passing through silica gel, anhydrous $Mg(ClO_4)_2$ and P_2O_5, and then deoxidized by passing through copper wool at 723 K and titanium granules at 1100 K. High purity oxygen was purified by passing over CuO at 800 K to convert residual CO to CO_2 and H_2 to H_2O. Passing over NaOH pellets then removed the CO_2 from oxygen. The oxygen was further dried using the same chemicals as described above for argon gas.

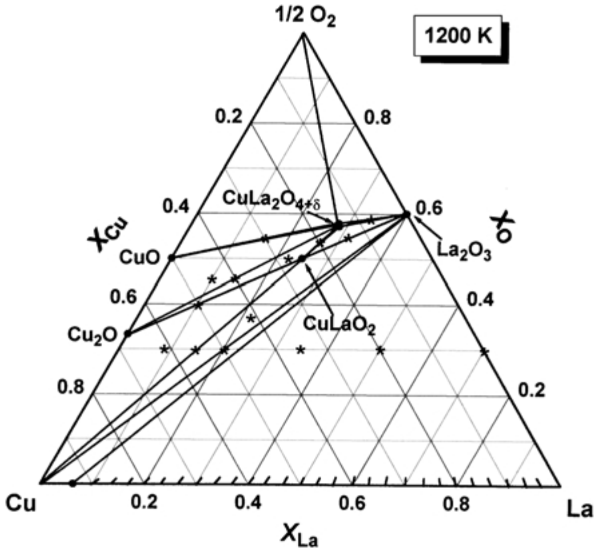

Figure 2 Phase relations in the system Cu-La-O at 1200 K. The average composition of the analyzed samples is shown by the symbol ∗.

2.2. Phase relations in the system Cu-La-O

Phase relations at 1200 K were established by equilibrating different mixtures of metals, alloys and oxides for ~450 ks. Preliminary experiments indicated that ~300 ks were sufficient to attain equilibrium. Samples representing 15 compositions inside the ternary triangle were investigated. The average compositions of the samples used in this study are shown in Fig. 2. The samples containing metallic phases were equilibrated in closed molybdenum containers kept under pre-purified argon gas flowing at a rate of 3 ml/s. Oxide mixtures, containing copper in lower valent state, were equilibrated in closed zirconia crucibles, which were placed in evacuated quartz ampoules at a pressure of ~0.1 Pa. Oxide mixtures containing copper in divalent and lanthanum in trivalent states were equilibrated in pure oxygen at a pressure of 0.1 MPa. After equilibration samples were quenched in liquid nitrogen or chilled mercury. Optical microscope, scanning electron microscope (SEM) and powder X-ray diffraction (XRD) were used for phase identification of quenched samples. Phase compositions were determined using energy dispersive analysis of X-rays (EDX) and chemical analysis. To check for the attainment of equilibrium, samples of same overall composition were prepared using different starting materials. The approach to equilibrium from different directions was thus verified.

To measure oxygen nonstoichiometry of $CuLa_2O_{4+\delta}$, single-phase samples suspended on a thermobalance were equilibrated in $Ar + O_2$ mixtures at 1200 K for ~450 ks. The mixtures were prepared by mixing metered streams of the two gases for $1.0 > (P_{O_2}/P^o) > 0.01$. An electrochemical pump based on stabilized-zirconia was used to set oxygen partial pressures below 10^{-2} in argon gas. The oxygen partial pressure in the gas was also measured with a solid state sensor. The oxygen content of the solid sample after equilibration was determined from mass loss on reduction with $Ar + H_2$ (2 : 1) mixture in situ. The final readings of the thermobalance were recorded after reduction under pre-purified argon gas $(P_{O_2}/P^o) < 10^{-8}$. This procedure permitted the gradual desorption of water molecules from the La_2O_3 formed during reduction. Buoyancy correction was applied using density of gases. Another set of samples equilibrated at 1200 K was quenched to room temperature for determination of the valence state of copper by iodometric titration.

2.3. Emf measurements

The reversible emf of the following cells were measured as a function of temperature in the range from 950 to 1300 K:

$$\text{Pt, Cu} + \text{CuLaO}_2 + \text{La}_2\text{O}_3 \| (\text{Y}_2\text{O}_3)\text{ZrO}_2 \| \text{Cu} + \text{Cu}_2\text{O, Pt} \quad \text{(I)}$$

$$\text{Pt, La}_2\text{O}_3 + \text{CuLaO}_2 + \text{CuLa}_2\text{O}_4 \| (\text{Y}_2\text{O}_3)\text{ZrO}_2 \| \text{O}_2(0.1\ \text{Mpa}), \text{Pt} \quad \text{(II)}$$

$$\text{Pt, Cu}_2\text{O} + \text{CuLaO}_2 + \text{CuLa}_2\text{O}_4 \| (\text{Y}_2\text{O}_3)\text{ZrO}_2 \| \text{O}_2(0.1\ \text{Mpa}), \text{Pt} \quad \text{(III)}$$

The cells are written such that the right-hand electrodes are positive. They were designed based on phase relations established in this study. Cell-I was fashioned such that the emf is directly related to the standard Gibbs energy of formation of $CuLaO_2$ from its component oxides Cu_2O and La_2O_3. The nature of phase relations in the system Cu-La-O does not permit the creation of a cell that will directly yield the Gibbs energy of formation of $CuLa_2O_4$ from CuO and La_2O_3. This information can be obtained indirectly by combining the emf of cell-I with the emf of either cell-II or cell-III and the standard Gibbs energy change for the oxidation of Cu_2O to CuO. Alternatively, emfs of cells II and III can be combined with the Gibbs energy change for the oxidation of Cu_2O to CuO to generate the Gibbs energies of formation of the two ternary oxides. Thus, measurements on three cells provide for a check of internal consistency.

The solid-state cell-I had a two-electrode design similar to that described by Jacob *et al.* [22]. The simpler two-electrode design was adequate for measurements on cell-I since the emf, and consequently the oxygen potential gradient across the electrolyte, was relatively small. The electrodes were prepared by mixing fine powders of metal and oxides. The average particle size of the powders used to prepare the electrodes varied from 3 to 15 μm. The compacted electrode pellets were pre-sintered in vacuum 1050 K. The electrolyte tube physically separated reference electrode compartment from the measuring electrode. Separate streams of pure, dry Ar gas were passed over each electrode. A Pt /Pt-13% Rh thermocouple monitored the temperature of the cell, and the emf was measured using a high impedance digital voltmeter. The reversibility of the emf was checked by microcoulometric titration in both directions. In each case, the emf returned to the original value. Temperature cycling confirmed the attainment of equilibrium during emf measurements. The emf was also independent of the flow rate of argon gas over the electrodes in the range 1.5 to 4 ml/s.

For measurements on cells II and III, a novel cell design incorporating a buffer electrode [19–21] was used since the emfs were relatively large. A schematic diagram of the three-electrode cell assembly is given in Fig. 3. The novel three-electrode cell can be represented as:

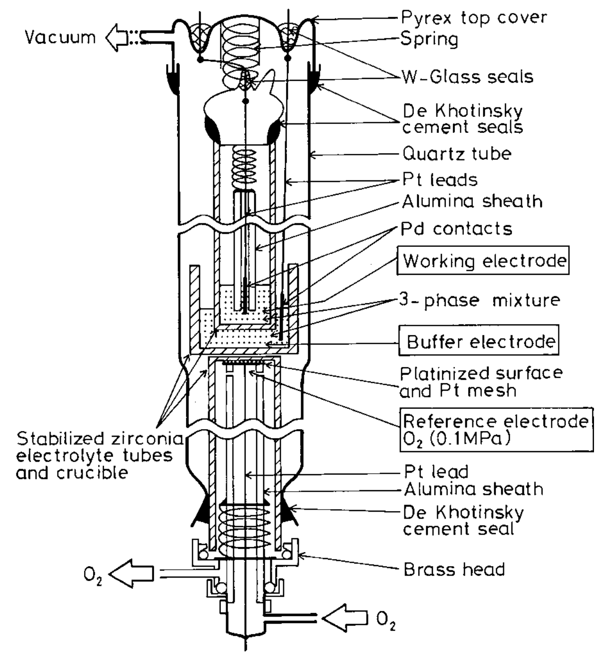

Figure 3 Schematic diagram of the new solid state cell with the buffer electrode.

Measuring Electrode	$(Y_2O_3)ZrO_2$	Buffer Electrode	$(Y_2O_3)ZrO_2$	Reference Electrode
$O_2(P'_{O_2})$, Pt	No flux	$O_2(P''_{O_2})$, Pt	←	O_2(0.1 MPa), Pt
		$P'_{O_2} \approx P''_{O_2}$	O^{2-}	

It consisted of three distinct compartments, separated by two impervious yttria-stabilized zirconia tubes each closed at one end. The measuring and reference electrodes were contained inside separate zirconia tubes. When the difference in the chemical potential of oxygen between these electrodes is substantial, there is always a small flux of oxygen through the zirconia electrolyte separating them, even in the absence of physical porosity [17, 18]. The electrochemical permeability is caused by the coupled transport of oxygen ions and electrons (or holes) in the solid electrolyte under the oxygen potential gradient. Only opposing it with an external dc voltage, which is exactly equivalent to the oxygen chemical potential difference, can stop this flow of oxygen [23].

The electrochemical flux of oxygen would have caused polarization of multiphase solid electrodes. The chemical potential of oxygen in the micro-system near the solid electrode/electrolyte interface would have been altered because of the semi-permeability of the electrolyte to oxygen. The buffer electrode, introduced between reference and measuring electrodes was designed to act as a sink for the oxygen flux and prevent the flux from reaching the measuring electrode. The buffer electrode was maintained at an oxygen chemical potential close to that of the measuring electrode. Since there was no significant difference between the chemical potentials of buffer and measuring electrodes, driving force for transport of oxygen through the zirconia tube separating these electrodes did not exist. The measuring electrode therefore remained non-polarized. Pure oxygen gas at a pressure of 0.1 MPa flowing over a platinized surface of zirconia constituted the primary reference standard for oxygen potential and formed a non-polarizable electrode. Thus, the three-electrode design of the cell prevented error in emf caused by polarization of the measuring electrode. The correct cell emf (E) is measured between the reference and measuring electrodes. Measuring separately the emf between the reference and the buffer electrodes ($E_{\text{r-b}}$), and that between the buffer and measuring electrodes ($E_{\text{b-m}}$), assessed the magnitude of the polarization effect ($E_p = E - E_{\text{r-b}} - E_{\text{b-m}}$). The value of $E_{\text{b-m}}$ was always less than 1 mV. In this study the polarization effect reduced the emf between 7 to 9 mV for cells II and III. The details of the cell assembly were the same as those reported earlier [19–21].

The measuring electrodes were chosen based on the phase relations established at 1200 K for the ternary Cu-La-O. The measuring and buffer electrodes of cells II and III were kept under static vacuum during measurements since their equilibrium oxygen partial pressures are relatively high. When an inert gas flow was maintained over these electrodes at high temperature, oxygen was removed by entrainment in the gas. The static vacuum arrangement was found to be better than the inert gas flow system. Excess of the ternary oxide $CuLa_2O_4$ was used in the preparation of each electrode, since a small amount of this phase had to decompose initially to establish the equilibrium oxygen pressure in the apparatus. The electrode mixture was rammed against the closed end of a stabilized zirconia tube with a Pt lead embedded in the mixture.

3. Results and discussion

3.1. Phase diagram

Phase relations in the system Cu-La-O at 1200 K composed from the results of this study are shown in Fig. 2. Along the binary La-O, one stable ternary oxide is identified: La_2O_3. Two oxides, Cu_2O and CuO with cuprite and tenorite structures respectively, were present in the binary system Cu-O. A liquid alloy phase field and a two-phase region $\{Cu + Cu_{1-x}La_x(l)\}$, characterize the binary Cu-La at 1200 K. Two ternary oxides, $CuLaO_2$ and $CuLa_2O_{4+\delta}$, were identified inside the ternary triangle. The Cu/La ratio in the two compounds determined using EDX were 1.00 (±0.02) and 2.00 (±0.02). Copper is monovalent in $CuLaO_2$ and divalent in $CuLa_2O_4$; lanthanum is in the trivalent state in both compounds. The oxygen content of single phase $CuLaO_2$ equilibrated at 1200 K, determined by reductive decomposition in $Ar + H_2$ (2 : 1) mixture, was 2.00 (±0.01) per formula unit. Values of the nonstoichiometric parameter (δ) in $CuLa_2O_{4+\delta}$ at different oxygen partial pressures are given in Table I along with hole concentration (h) of quenched samples obtained by iodometric titration. There is a small systematic difference between TGA and titration results; the difference increases with nonstoichiometry. This difference is probably caused by the inability to freeze high-temperature equilibrium during quenching. *In situ* TGA measurements are more accurate. However, if the differences are real, it would imply that the average oxidation state of the intercalated oxygen reduces from a value of −2 close to stoichiometry to about −1.7 in pure oxygen at 1200 K. At large deviations from stoichiometry, the inserted oxygen may take one of many forms, O_2°, O^-, O_2^-, or O_2^{2-}, with charge balance requiring the formation of Cu^{3+}. The relative concentration of polyoxide species is expected to increase with decreasing temperature. In support of this, Li *et al.* [24] have shown that for $CuLa_2O_{4+\delta}$ samples annealed at 383 K, $[h] = 2\delta$ at small deviations from stoichiometry (up to $\delta \leq 0.03$), and $[h] = 1.3\,\delta + 0.019$ for $0.03 < \delta < 0.11$.

TABLE I Nonstoichiometric parameter (δ) and hole concentration (h) of $CuLa_2O_{4+\delta}$ at different partial pressures of oxygen at 1200 K

$\log P_{O_2}$	δ (TGA/H_2 Reduction)	h (Iodometric titration)
0	0.120	0.201
−0.276	0.108	0.186
−0.983	0.0823	0.137
−1.317	0.0724	0.124
−1.896	0.0579	0.107
−2.359	0.0485	0.092
−2.804	0.0409	0.081
−3.201	0.0351	0.070
−3.827	0.0276	0.055
−4.326	0.0228	0.046

The variation of δ with oxygen partial pressure at 1200 K can be expressed by the relation:

$$\log\delta = -0.915 + 0.169\log\left(P_{O_2}/P^\circ\right)(\pm 0.04) \quad (1)$$

It is clearly established that the compound contains excess oxygen, the concentration of which increases with 1/6 power of P_{O_2}. This indicates the presence of oxygen interstitials in agreement with neutron scattering experiments [5] as shown in Fig. 1. Magnetic measurements have also been interpreted in this manner [25]. Studies on electrical conductivity, thermoelectric power and Hall-effect indicate that the concentration of electron holes follow a 1/6 power law dependence on P_{O_2} [3, 4]. On the basis of these results the oxygen insertion at high temperatures can be described by the defect reaction:

$$1/2\,O_2 + V_i \rightarrow O_i'' + 2\,h^\bullet \quad (2)$$

It is known that $CuLa_2O_4$, which is an antiferromagnetic insulator with distorted K_2NiF_4 layered structure, becomes a prototype high-T_c superconductor with onset T_c as high as 45 K in bulk samples [26] and 60 K in thin films [27] upon anion doping.

Pure copper metal was found to coexist with La_2O_3. Six three-phase fields involving condensed phases were identified. They are:

(i) $Cu + Cu_{0.94}La_{0.06}(l) + La_2O_3$,
(ii) $Cu + La_2O_3 + CuLaO_2$,
(iii) $Cu + Cu_2O + CuLaO_2$,
(iv) $CuLaO_2 + CuLa_2O_{4+\delta} + La_2O_3$,
(v) $Cu_2O + CuLaO_2 + CuLa_2O_{4+\delta}$, and
(vi) $Cu_2O + CuO + CuLa_2O_{4+\delta}$.

The phases $CuLa_2O_4$ and Cu did not coexist at equilibrium. Similarly, there was no tie-line connecting

$CuLaO_2$ and CuO. Solid solubility between the oxides was negligible (<0.2 mol%) at 1200 K. According to the phase rule, each three-phase field is associated with zero degree of freedom at constant temperature. Hence, each of these phase fields is characterized by a unique oxygen partial pressure. The activity of La in the liquid alloy and the standard Gibbs energy of formation of La_2O_3 determine the oxygen potential corresponding to the first three-phase field. Thermodynamic considerations require oxygen potential to increase in the phase fields traversed when one proceeds in a straight line from any point on the binary Cu-La towards the oxygen apex in Fig. 2.

The compounds $Cu_2La_2O_5$ and $Cu_7La_8O_{19}$ were not detected at 1200 K. Compounds belonging to the Ruddlesden-Popper series ($A_{n+1}B_nO_{3n+1-\delta}$) [28] were also not identified. At low temperatures ($T < 760$ K), $CuLaO_2$ allows intercalation of oxygen to produce a phase with the composition $LaCuO_{2.65}$, which essentially retains the delafossite structure [29]. As temperature is increased gradually above 800 K in pure oxygen, this metastable phase decomposes producing initially an amorphous or poorly crystallized phase and eventually a mixture of $CuLa_2O_4$ and CuO [29].

3.2. Thermodynamic properties

At temperatures above 1285 K, presence of a liquid phase was detected at the measuring electrode of cell I. The reversible emf of cell I below 1285 K is displayed in Fig. 4 as a function of temperature. The least-squares regression analysis gives the expression;

$$E_I/\text{mV} = 44.94 - 0.0137\,(T/\text{K}) \quad (\pm 0.44) \qquad (3)$$

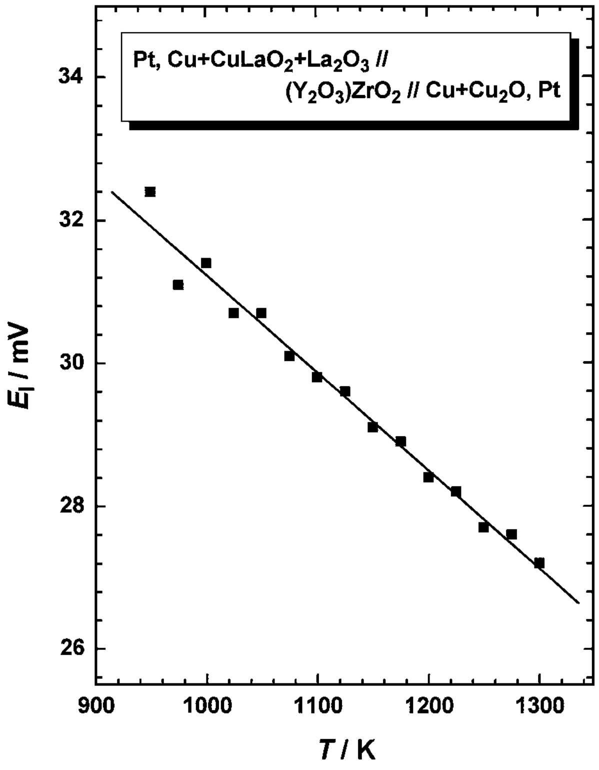

Figure 4 The reversible emf of cell I as a function of temperature.

The electrochemical reaction at the right-hand electrode of cell I is,

$$1/2\,Cu_2O + e^- \rightarrow Cu + 1/2\,O^{2-} \qquad (4)$$

At the left-hand electrode, the electrochemical reaction is,

$$Cu + 1/2\,O^{2-} + 1/2\,La_2O_3(\text{A rare-earth}) \rightarrow CuLaO_2 + e^- \qquad (5)$$

The virtual cell reaction, obtained by combining the two half-cell reactions, is;

$$1/2\,Cu_2O + 1/2\,La_2O_3(\text{A rare-earth}) \rightarrow CuLaO_2 \qquad (6)$$

The emf of cell I is directly related to the standard Gibbs energy change for reaction (6):

$$\Delta_{r(6)}G^\circ/\text{J}\cdot\text{mol}^{-1} = -FE_I = -4335 + 1.32(T/\text{K})\ (\pm 42) \qquad (7)$$

where $F = 96\ 485$ J/V · mol is the Faraday constant. The standard Gibbs energy of formation of $CuLaO_2$ from its component oxides Cu_2O (cuprite) and La_2O_3 is exactly the Gibbs energy change given by (7). As shown in Fig. 5, the Gibbs energy of formation of $CuLaO_2$ from component binary oxides obtained in this study is in reasonable agreement with values reported by Chandrasekharaiah *et al.* [11]. Although the value reported by Petrov *et al.* [12] agrees with that obtained

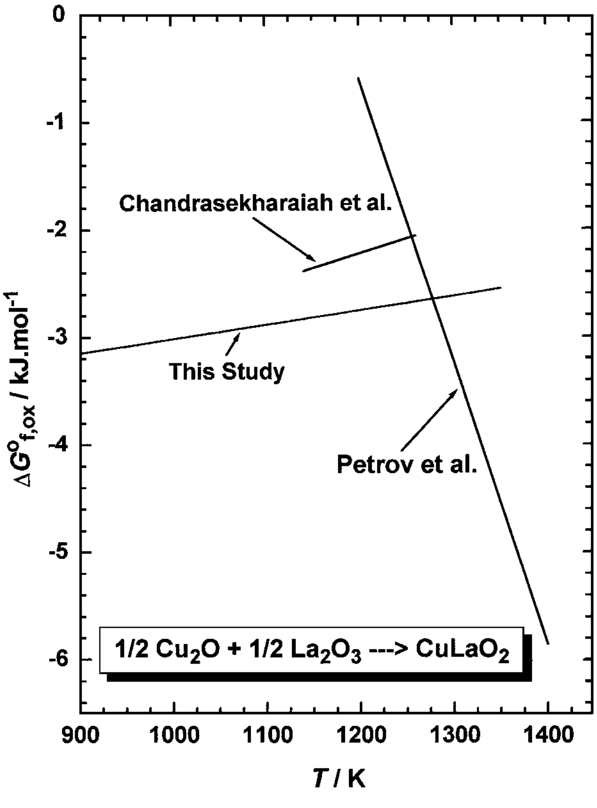

Figure 5 Temperature dependence of the standard Gibbs energy of formation of $CuLaO_2$ from its component binary oxides—comparison of the data obtained in this study with those given in the literature [11, 12].

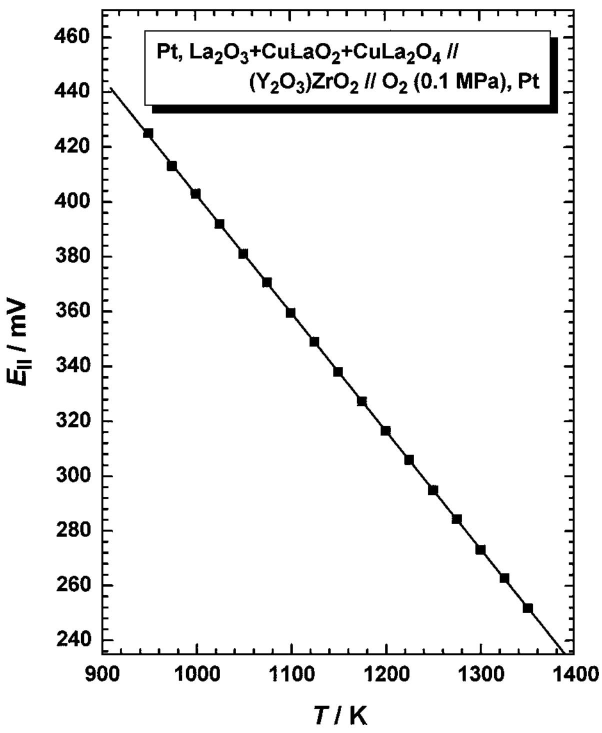

Figure 6 The reversible emf of cell II as a function of temperature.

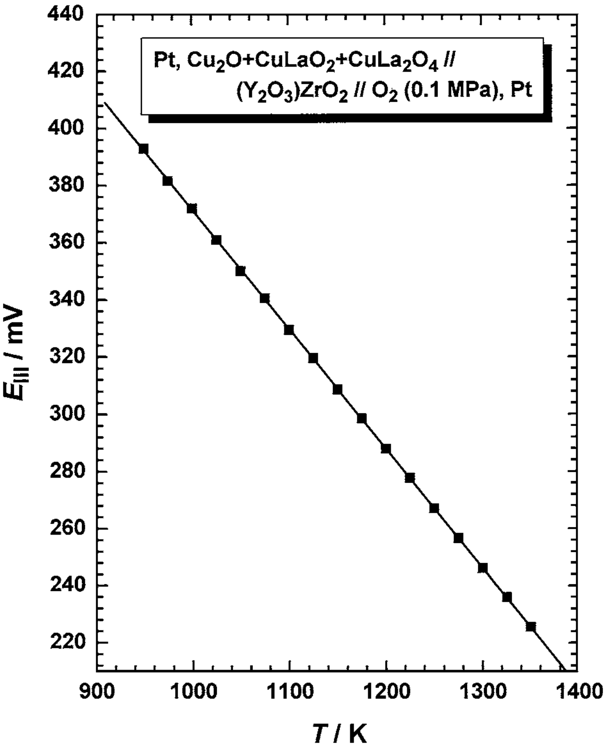

Figure 7 The reversible emf of cell III as a function of temperature.

in this study at 1285 K, the slopes of the curves have opposite sign. There is no reason to expect large entropy stabilization (26.25 J/mol · K with respect to the component binary oxides) of the delafossite compound. According to Petrov *et al.* [12], $CuLaO_2$ is unstable below 1183 K.

The oxygen potential corresponding to the equilibrium between the three phases Cu, La_2O_3 and $CuLaO_2$ can be computed from the emf of cell-I and the oxygen potential for the Cu + Cu_2O reference [30]. The oxygen potential is defined by:

$$4\,Cu + O_2 + 2\,La_2O_3(\text{A rare-earth}) \rightarrow 4\,CuLaO_2 \qquad (8)$$

$$\Delta\mu_{O_2}/J \cdot mol^{-1} = -352\,729 + 148.68\,(T/K)\,(\pm 400) \qquad (9)$$

The major source of uncertainty in (9) comes form thermodynamic data for pure Cu_2O $\{\Delta_f G^{\circ}/J \cdot mol^{-1} = -167\,690 + 71.60\,(T/K)\,(\pm 420)\}$ [30].

The temperature dependence of the reversible emfs of cells II and III are shown in Figs 6 and 7. The emfs are linear functions of temperature. If the compounds $Cu_2La_2O_5$ and $Cu_7La_8O_{19}$ had formed during the high temperature experiments in the temperature range 1260–1375 K, a change of slope would have been expected. The emfs of cells II and III thus suggest that the two compounds are unstable relative to a mixture of CuO and $CuLa_2O_4$. Further discussion on the stability of $Cu_2La_2O_5$ and $Cu_7La_8O_{19}$ is given at the end of this section. The least-squares regression analysis gives:

$$E_{II}/mV = 834.2 - 0.4314\,(T/K)\,(\pm 0.54) \qquad (10)$$

$$E_{III}/mV = 789.3 - 0.4177\,(T/K)\,(\pm 0.66) \qquad (11)$$

The emf of cell-II directly gives the oxygen potential for three-phase equilibrium defined by the reaction:

$$4\,CuLaO_2 + 2\,La_2O_3(\text{A rare-earth}) + O_2 \rightarrow 4\,CuLa_2O_4 \qquad (12)$$

The oxygen chemical potential corresponding to the three-phase field $CuLaO_2 + CuLa_2O_4 + La_2O_3$ is given by:

$$\Delta\mu_{O_2}/J \cdot mol^{-1} = -4FE_{II} = -321\,950 + 166.49\,(T/K)\,(\pm 210) \qquad (13)$$

The oxygen potential measured in this study is compared with those reported by Chandrasekharaiah *et al.* [11] and Petrov *et al.* [12] and in Fig. 8. The result of this study agrees exactly with that of Chandrasekharaiah *et al.* [11] at 1200 K; but the slopes of the lines differ significantly. The maximum deviation in chemical potential is ~4 kJ/mol. Chandrasekharaiah *et al.* [11] used Ni + NiO as the reference electrode in their measurements. The data of Petrov *et al.* [12], obtained using air as the reference electrode, are consistently more positive than that obtained in this study; the difference being ~4.5 kJ/mol. It is quite likely that this error is caused by polarization of their three-phase electrodes as a result of the electrochemical flux of oxygen through the solid electrolyte from the reference side. The oxygen potentials measured in this study using the new cell design with buffer electrodes are more reliable.

The emf of cell-III directly gives the oxygen potential for three-phase equilibrium defined by the reaction:

$$8\,CuLaO_2 + O_2 \rightarrow 4\,CuLa_2O_4 + 2\,Cu_2O \qquad (14)$$

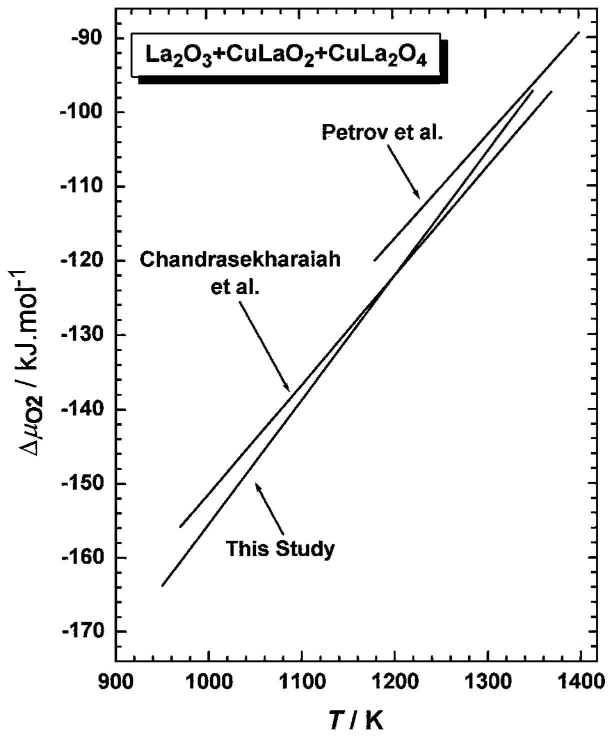

Figure 8 Comparison of the oxygen chemical potential measured in this study for the three-phase field $CuLa_2O_4 + CuLaO_2 + La_2O_3$ with information in the literature [11, 12].

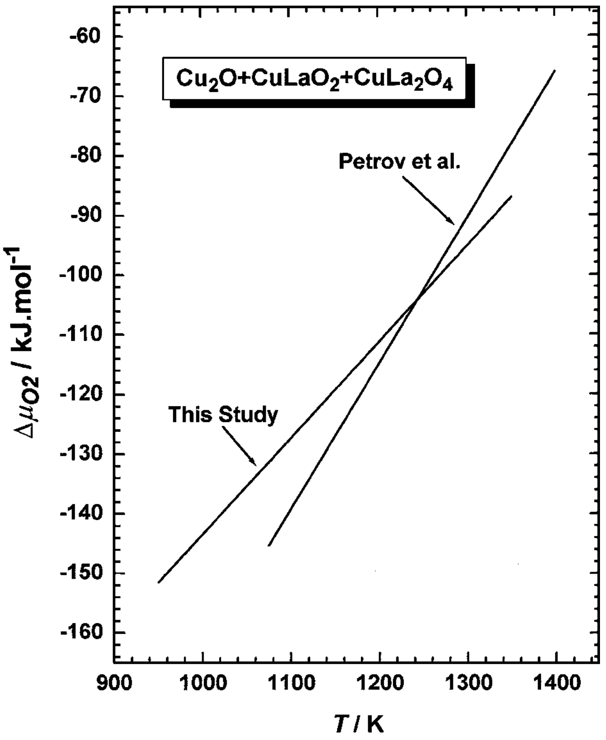

Figure 9 Comparison of the oxygen chemical potential measured in this study for the three-phase field $Cu_2O + CuLaO_2 + CuLa_2O_4$ with data in the literature [12].

$$\Delta\mu_{O_2}/\mathrm{J\cdot mol^{-1}} = -4\,\mathrm{F}E_{III} = -304\,620 + 161.21\,(T/\mathrm{K})\ (\pm 255) \qquad (15)$$

Fig. 9 compares the values obtained in this study with those of Petrov *et al.* [12]. The results of this study agree with the measurements of Petrov *et al.* [12] for the $CuLa_2O_4 + CuLaO_2 + Cu_2O$ equilibrium at ~1245 K. But the slopes differ significantly. For a reaction involving the consumption of one mole of oxygen gas, the magnitude of the entropy change that is deduced from the data of Petrov *et al.* [12] is unreasonably large.

The oxygen potential corresponding to $Cu_2O + CuO$ has been reported in an earlier publication [31] as;

$$\Delta\mu_{O_2}/\mathrm{J\cdot mol^{-1}} = -260\,889 + 187.82\,(T/\mathrm{K})\ (\pm 420) \qquad (16)$$

Combining Equation 16 with 7 and 13, standard Gibbs energy of formation of $CuLa_2O_4$ from component binary oxides CuO and La_2O_3 is obtained:

$$CuO + La_2O_3(\text{A rare-earth}) \rightarrow CuLa_2O_4 \qquad (17)$$

$$\Delta_{f,ox}G^o/\mathrm{J\cdot mol^{-1}} = -19\,598 - 4.04\,(T/\mathrm{K})\ (\pm 240) \qquad (18)$$

Almost identical values for $CuLa_2O_4$ are obtained by combining Equations 16, 7 and 15, thus demonstrating that small difference in oxygen content of $CuLa_2O_{4+\delta}$ present in different phase fields does not significantly affect its the Gibbs energy of formation. It is interesting to note that the stability of the compound with respect to its component binary oxides increases with temperature. The temperature-independent term in Equation 18 gives the enthalpy of formation of $CuLa_2O_4$ from its component oxides as −19.6 (±0.6) kJ/mol at an average temperature of 1150 K. This compares well with the calorimetric value of −19.30 (±4.7) kJ/mol at 973 K obtained by Bularzik *et al.* [13]. The standard Gibbs energy of formation of $CuLa_2O_4$ obtained in this study is compared in Fig. 10 with other values reported in the

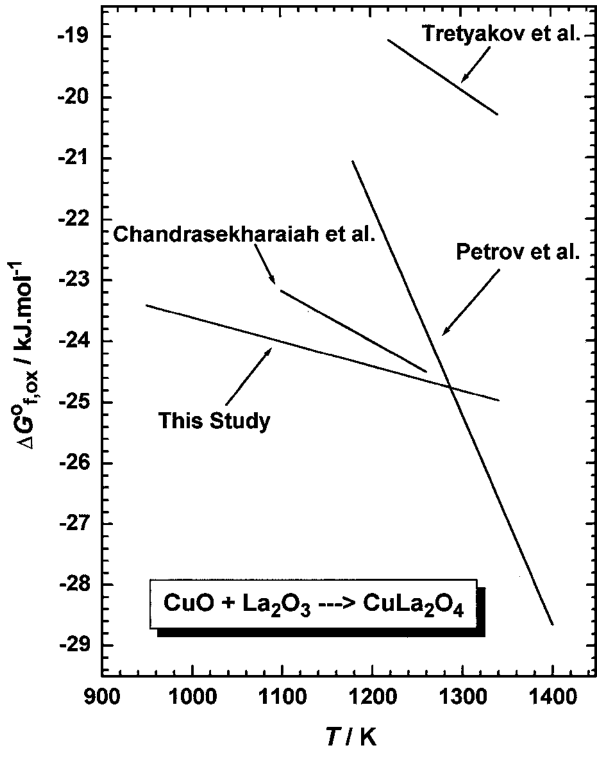

Figure 10 Temperature dependence of the standard Gibbs energy of formation of $CuLa_2O_4$ from its component binary oxides—comparison of the data obtained in this study with those given in the literature [10–12].

literature. The present results are in reasonable agreement with those of Chandrasekharaiah *et al.* [11]. The temperature dependence of the Gibbs energy obtained from Petrov *et al.* [12] appears to be incorrect. The results of Tretyakov *et al.* [10] are considerably more positive. Since they employed a non-equilibrium mixture of $Cu_2O + La_2O_3 + CuLa_2O_4$ at their measuring electrode (refer to Fig. 3), their results are not considered to be reliable.

It is useful to consider the stability of $La_2Cu_2O_5$ in the light of trends in thermodynamic data for $Ln_2Cu_2O_5$ (Ln = Tb, Dy, Ho, Er, Tm, Yb, Lu, Y), which have been critically assessed recently [32]. The structure of $Ln_2Cu_2O_5$ (Ln = Tb-Lu, Y) compounds belongs to the noncentrosymmetric orthorhombic space group $Pna2_1$, containing distorted LnO_6 and CuO_5 polyhedra. The compounds have a positive enthalpy of formation and are entropy stabilized at high temperatures. The standard Gibbs energy of formation of these compounds from the binary oxides becomes less negative with increasing ionic radius of Ln^{3+} ion. Based on this trend, $La_2Cu_2O_5$ with the same structure would not be stable at around 1300 K. However, $La_2Cu_2O_5$ synthesized by Cava *et al.* [15] and Norrestam *et al.* [16] has a large monoclinic unit cell ($C2/c$). The structure consists of thin ribbons of $CuLa_2O_4$ sandwiched between Cu-O planes of complex low-dimensional geometry; La is coordinated by 9 oxygens, and Cu by 4 and 6 oxygens. Gibbs energies of a compound in two different crystal structures generally differ by only a few kJ/mol. If $La_2Cu_2O_5$ has to be stable phase in the system Cu-La-O at 1300 K, its standard Gibbs energy of formation from Ln_2O_3 and CuO should be lower (more negative) than −24.85 kJ/mol. Such a large stabilization is difficult to obtain by a change in crystal structure. It may therefore be concluded that $La_2Cu_2O_5$ is a metastable compound. Its formation under very restricted conditions at high temperature may be the consequence of Ostwald's step rule, according to which phases of higher entropy form first during the reaction between binary oxides. The decay of the metastable phase to the stable assemblage is often a markedly slow process.

3.3. Oxygen potential diagram

The oxygen potential diagram for the system Cu-La-O at 1200 K, composed from the results of this study and data from the literature on binary oxides [30, 31, 33] and alloys [34], is shown in Fig. 11. The composition of a component is normally designated by its mole fraction, which is obtained by dividing the number of moles of the component by the sum of moles of all components. The normalized mole fraction, used as the composition variable in the chemical potential diagram, is obtained by removing the component (in the present case, oxygen), the chemical potential of which is being plotted, from the summation. The normalized mole fraction on the X-axis is identical to the cationic fraction of La ($\eta_{La}/\eta_{Cu} + \eta_{La}$) in oxides, where η_i represent moles of component i. With this choice of composition variable, the chemical potential of oxygen becomes and independent variable. However, since oxygen is not included in the composition parameter, information on oxygen nonstoichiometry cannot be displayed on the diagram. Nevertheless, the diagram provides useful information on the oxygen potential range for the stability of various phases. The diagram is complimentary to the conventional Gibbs triangle representation of phase relations in the ternary Cu-La-O (Fig. 2). When three condensed phases and a gas phase coexist at equilibrium in the ternary Cu-La-O, the system is mono-variant; at a fixed temperature, three condensed phases coexist only at a unique partial pressure of oxygen. Horizontal lines on the diagram therefore represent equilibria involving three condensed phases.

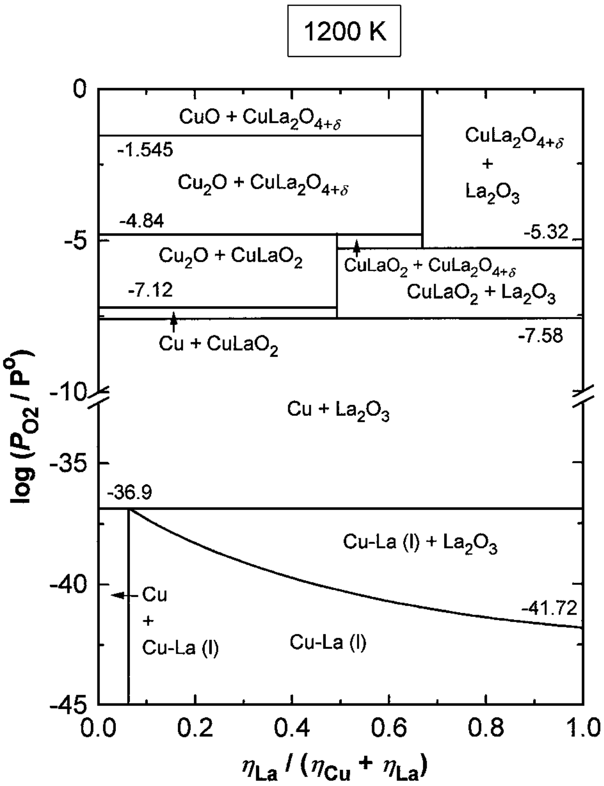

Figure 11 Oxygen chemical potential diagram for the system Cu-La-O at 1200 K composed from the results obtained in this study and data on binary phases reported in the literature [30, 31, 33, 34].

Chemical potentials of oxygen corresponding to the equilibria $Cu + Cu_2O$, $Cu_2O + CuO$ were calculated from the available thermodynamic data on binary oxides [30, 31]. For the alloy Cu-La, Gibbs energy of mixing (ΔG^{m}) at 1200 K has been modeled using Redlich-Kister equation by Du *et al.* [34]

$$\Delta G^{m} = x_{Cu}x_{La}\sum_{i=0}^{i=2} L_i(x_{Cu} - x_{La})^i \tag{19}$$

$$\overline{G}^{E}_{La} = x^2_{Cu}[L_0 - L_1(3x_{La} - x_{Cu}) + L_2(x_{La} - x_{Cu})(5x_{La} - x_{Cu}) + ...] \tag{20}$$

where $L_0 = -34\,940$ J/mol, $L_1 = -29\,320$ J/mol and $L_2 = -8\,995$ J/mol at 1200 K. Substituting these values in (20), the partial excess Gibbs energy and activity of La in the liquid alloy Cu-La were calculated. From the standard Gibbs energy of formation of La_2O_3 [33] and activity of La in the liquid alloy, partial pressure of oxygen for the two-phase field Cu-La (l) + La_2O_3 was obtained at 1200 K:

$$\log\left(P_{O_2}/P^{o}\right) = [\{(2/3)\Delta_f G^{o}(La_2O_3)/2.303\,RT\} \\ -(4/3)\log a_{La}] \qquad (21)$$

Experimental measurement of the chemical potential of oxygen for the equilibrium involving Cu-La (*l*) and Ln_2O_3 is difficult since the partial pressures of oxygen range from $\log(P_{O_2}/P^{o}) = -41.72$ to -36.90 at 1200 K, well below the domain of application of current experimental techniques. The values of (P_{O_2}/P^{o}) for the three-phase fields starting from $Cu + CuLaO_2 + La_2O_3$ to $Cu_2O + CuLaO_2 + CuLa_2O_{4+\delta}$ are based on electrochemical measurements reported in this article.

4. Conclusions

The phase diagram for the ternary system Cu-La-O has been experimentally determined at 1200 K by phase analysis of quenched samples using XRD, SEM and EDX. There are two stable ternary oxides in the system $CuLaO_2$ and $CuLa_2O_{4+\delta}$. The excess oxygen in lanthanum cuprate is accommodated in interstitial sites. The ternary oxides, $Cu_2La_2O_5$ and $Cu_7La_8O_{19}$, which have been synthesized from CuO and La_2O_3 in narrow ranges of temperature and oxygen partial pressure, are metastable phases.

Based on the isothermal phase relations, solid-state cells were designed for the measurement of thermodynamic properties of the ternary oxides. Although measurements on two solid-state cells were sufficient to generate the data, three cells were actually used in order to provide a crosscheck on derived data. A novel three-electrode design, with a buffer electrode placed between the reference and measuring electrodes, minimized errors due to polarization during measurement of oxygen potential in the three-phase fields relative to pure diatomic oxygen gas as the reference. The standard Gibbs energies of formation for the ternary oxides $CuLaO_2$ and $CuLa_2O_4$ obtained in the present study are discussed in comparison with values reported in the literature. An oxygen chemical potential diagram is constructed for the ternary system Cu-La-O at 1200 K from the results obtained in the present study and data available in the literature. The stability domain of alloys and oxides are clearly shown on the diagram as a function of oxygen potential.

References

1. B. VON GRANDE, HK. MÜLLER BUSCHBAUM and M. SCHWEIZER, *Z. Anorg. Allg. Chem.* **428** (1977) 120.
2. E. J. OPILA and H. L. TULLER, *Mater. Res. Soc. Symp. Proc.* **209** (1991) 867.
3. S. NISHIYAMA, N. KIEDA, K. SHINOZAKI, M. KATO and N. MIZUTANI, *J. Ceram. Soc. Jpn. Inter. Ed.* **97** (1989) 1114.
4. N. KIEDA, S. NISHIYAMA, K. SHINOZAKI and N. MIZUTANI, *Solid State Ionics* **49** (1991) 85.
5. C. CHAILLOUT, S. W. CHEONG, Z. FISH, M. S. LEHMANN, M. MAREZIO, B. MOROSIN and J. E. SCHIRBER, *Physica* C **158** (1989) 183.
6. B. O. WELLS, Y. S. LEE, M. A. KASTNER, R. J. CHRISTIANSON, R. J. BIRGENEAU, K. YAMADA, Y. ENDOH and G. SHIRANE, *Science* **277** (1997) 1067.
7. B. O. WELLS, R. J. BIRGENEAU, F. C. CHOU, Y. ENDOH, D. C. JOHNSTON, M. A. KASTNER, Y. S. LEE, G. SHIRANE, J. M. TRANQUADA and K. YAMADA, *Z. Phys.* B **100** (1996) 535.
8. J. D. JORGENSON, B. DABROWSKI, S. PEI, D. G. HINK, L. SODERHOLM, B. MOROSIN, J. E. SCHIRBER, E. L. VENTURINI and D. S. GINLEY, *Phys. Rev.* B. **38** (1988) 11 337.
9. P. G. RADAELLI, J. D. JORGENSON, R. KLEB, B. A. HUNTER, F. C. CHOU and D. C. JOHNSTON, *ibid.* **49** (1994) 6239.
10. YU. D. TRETYAKOV, A. R. KAUL and N. V. MAKUKHIN, *J. Solid State Chem.* **17** (1976) 183.
11. M. S. CHANDRASEKHARAIAH, M. D. KARKHANAVALA and O. M. SREEDHARAN, *High Temp. Sci.* **11** (1979) 65.
12. A. N. PETROV, A. YU. ZUEV and V. A. CHEREPANOV, *Russ. J. Phys. Chem.* **62** (1988) 1613.
13. J. BULARZIK, A. NAVROTSKY, J. DICARLO, J. BRINGLEY, B. SCOTT and S. TRAIL, *J. Solid State Chem.* **93** (1991) 418.
14. K. SUN, J. H. CHO, F. C. CHOU, W. C. LEE, L. L. MILLER and D. C. JOHNSTON, *Phys. Rev.* B. **43** (1991) 239.
15. R. J. CAVA, T. SIEGRIEST, B. HESSEN, J. J. KRAJEWSKI, W. F. PECK, JR., B. BATTLOGG, H. TAKAGI, J. V. WASZCZAK and L. F. SCNEEMEYER, *J. Solid State Chem.* **94** (1991) 170.
16. R. NORRESTAM, M. NYGREN and J.-O. BOVIN, *Angew. Chem. Int. Ed. Engl.* **30** (1991) 864.
17. J. FOULTIER, P. FABRY and M. KLEITZ, *J. Electrochem. Soc.* **123** (1976) 204.
18. K. T. JACOB and T. MATHEWS, *Ind. J. Tech.* **28** (1990) 413.
19. K. T. JACOB and K. P. JAYADEVAN, *J. Mater. Chem.* **7** (1997) 2407.
20. *Idem.*, *Mater. Sci. Eng.* B **52** (1998) 134.
21. *Idem.*, *Chem. Mater.* **12** (2000) 1779.
22. K. T. JACOB, G. M. KALE, and G. N. K. IYENGAR, *Metall. Trans.* B **20B** (1989) 679.
23. K. T. JACOB and J. H. E. JEFFES, *Trans. Inst. Min. Metall., Sec.* C **80** (1971) C181.
24. Z. G. LI, H. H. FENG, Z. Y. YANG, A. HAMED, S. T. TING and P. H. HOR, *Phys. Rev. Lett.* **77** (1996) 5413.
25. D. C. JOHNSON, J. P. STOKES, D. P. GOSHORN and J. T. LEWANDOWSKI, *Phys. Rev.* B **36** (1987) 4007.
26. A. WALTIAUX, J. C. PARK, J. C. GRENIER and M. POUCHARD, *C. R. Acad Sci.* **310** (1990) 1047.
27. J. C. GRENIER, F. ARROUY, J. P. LOCQUET, C. MONROUX, M. POUCHARD, A. VILLESUZANNE and A. WALTIAUX, “Phase Separation in Cuprate Superconductors,” edited by E. Sigmund and K. A. Muller (Springer-Verlag, Berlin, 1994) p. 236.
28. S. N. RUDDLESDEN and P. POPPER, *Acta Crystallogr.* **11** (1958) 54.
29. R. J. CAVA, H. W. ZANDBERGEN, A. P. RAMIREZ, H. TAKAGI, C. T. CHEN, J. J. KRAJEWSKI, W. F. PECK JR., J. V. WASZCZAK, G. MEIGS, R. S. ROTH and L. F. SCNEEMEYER, *J. Solid State Chem.* **104** (1993) 437.
30. K. T. JACOB and J. H. E. JEFFES, *Trans. Inst. Min. Metall., Sec.* C **80** (1971) C32.
31. K. T. JACOB and C. B. ALCOCK, *J. Amer. Ceram. Soc.* **8** (1975) 192.
32. K. P. JAYADEVAN and K. T. JACOB, *High Temp. Mater. Process.* **19** (2000) 389.
33. L. B. PANKRATZ, Thermodynamic Properties of Elements and Oxides, U. S. Department of the Interior, Bureau of Mines Bull. 672, 1982, p. 214.
34. Z. DU, Y. XU and W. ZHANG, *J. Alloys and Compds.* **289** (1999) 88.

Received 14 February
and accepted 11 December 2001